# DENSITY MEASUREMENTS OF ENDOTHERMIC HYDROCARBON FUELS AT TEMPERATURES FROM 235 K to 353 K AND PRESSURES UP TO 4.09 MPA

Feng S., Bi Q.C*., Pan H., Liu Z.H., and Guo Y.J.
*Author for correspondence
State Key Laboratory of Multiphase Flow in Power Engineering,
Xi'an Jiaotong University,
No.28 Xianning West Road, Xi'an 710049,
China
E-mail: qcbi@mail.xjtu.edu.cn

## ABSTRACT

The densities of endothermic hydrocarbon fuels were measured covering the temperature from (235.0 to 353.0) K at pressures of (0.68,1.47, 3.06 and 4.09) MPa. The densitometer is based on the attenuation theory of gamma ray with a count rate mode. When the intensity of a gamma beam passes through fuels, it decreases exponentially. According to Beer−Lambert's law, densities of fuel were calculated through the different count rates and densities of referenced fluid. Pure hexane and a binary mixture of n-heptane and n-octane were adopted respectively to validate the reliability and accuracy of the densitometer. Results showed that the average absolute deviation(AAD) was lower than 0.32 % and the maximum absolute deviation(MAD) was within 0.67 %.

## NOMENCLATURE

| | | |
|---|---|---|
| $I$ | n/s | Intensity of incident radiation |
| $\mu/\rho$ | $m^2/kg$ | Mass absorption coefficient |
| $\rho$ | $kg/m^3$ | Density |
| $x$ | m | Distance between radiation source and detected scintillator |
| $\Phi$ | | Count rates |
| Subscripts | | |
| H | | High density fluid |
| L | | Low density fluid |
| m | | Measured fluid |
| exp | | Experimental data |
| ref | | Referenced data |

## INTRODUCTION

Trends in increasing aircraft speeds and engine efficiencies are increasing vehicle and engine heat loads. To manage the numerous heat loads efficiently, emerging cooling technologies proved to be prospective way. In all emerging cooling technologies, the regenerative cooling system using the "endothermic fuel" onboard to meet the cooling requirements attracts significant research interests [1-3]. In the regenerate cooling system, endothermic hydrocarbon fuels service not only as a source of heat through combustion but as a "heat sink" to remove waste heat from aircraft subsystems. To model the flow and heat transfer in this situation, it is important to know the thermophysical properties of the fuel as a function of temperature over the operational range.

Density is an important property required in the determination of different fluid properties. The densities of pure compound [4,5] and binary [6,7] and ternary mixtures [8] have been investigated by many researchers who use piezometer devices [9], vibrating tube densitometers [6,10] or a rapid-heating sealed-ampule technique [11]. For endothermic hydrocarbon fuels, Deng et al. [12] investigated the density of a typical endothermic hydrocarbon fuel (RP-3) at temperatures from 295.0 K to 796.0 K and at sub- and supercritical conditions using a mass conversion method. Yang et al [13] constructed a densitometer based on attenuation of gamma ray using a count mode and measured a kind of endothermic hydrocarbon fuel covering the temperature from (283.0 to 950.0) K at the supercritical pressures of (3.00 and 4.00) MPa. Densities of fuels have been measured at high temperatures and high pressures by some researchers. However, densities of fuel at temperatures below 273.0 K scarcely can be found in the open literatures.

In the present work, the densitometer based on the attenuation of gamma ray was remoulded covering the temperature below 273.0 K. The reliability and accuracy of the densitometer was verified strictly. Finally, the densities of endothermic hydrocarbon fuels were measured at temperatures of (235.0-353.0) K and at pressures of (0.68,1.47, 3.06 and 4.09) MPa.

## EXPERIMENTAL SYSTEM

A schematic diagram of the experimental system is shown in Figure 1. The fluid was driven by a constant volumetric pump with a supply capacity of 100 ml/min. A filter was installed before a mass flowmeter to protect devices from entrained impurity. The mass flowmeter was used to measure the mass flow rate and observe the stability of the fluid flow. A coiled tube was immersed in a liquid thermostat, which covered the temperature range of (235.0-353.0) K. The fluid flowed through the coiled tube to reach the measured temperatures and then flowed into the test section.

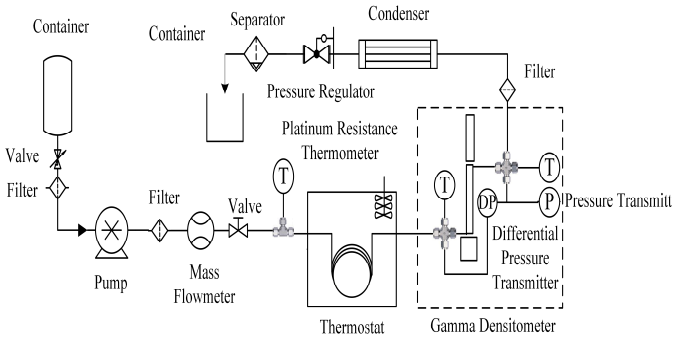


**Figure 1** A schematic diagram of the experimental system

In the test section, the inlet and outlet fuel temperatures were measured by two 4-wires platinum resistance thermometers. The qualitative temperature of fuel in the measurement was defined by the average of the two thermometers. A pressure transmitter was used to measure the work pressure, which was controlled by a back pressure regulator at the outlet. After testing, the fluid flowed through a condenser and was collected by a container. All the useful information was recorded by a data acquisition system.

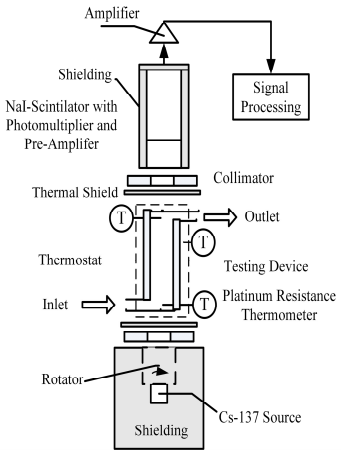


**Figure 2** Detailed configuration of the test section

The detailed configuration of the test section is shown in Figure 2. The Cs-137 source was chosen to radiate the gamma ray, which was controlled by a shielding rotator. The gamma ray crossed the test tube made of stain steel. The length, external and internal diameter of the test tube were 70 mm, 10mm, 8mm, respectively. The attenuated gamma ray was detected by NaI scintillator. The gamma pulses were transformed to the photoelectrons and then to the electrodes voltages. The amplifier was used to amplified the electrodes voltages. The amplified signal was analyzed by a multichannel analyzer and counted by a counter. Finally, the signal was conducted by an exclusive processing program and saved into a computer.

Two collimators were attached to the source and detector respectively, which was used to minimize the scattered photons contribution. To decrease the heat loss, the test tube was immersed in a gas thermostat. The temperature of the inside thermostat was equal to the average temperature of the inlet and outlet fluid. Through the experimental measurement, deviations of the inlet and outlet fluid temperature were below 0.1 K.

## MATERIALS

Pure hydrocarbon hexane, heptane and octane were all supplied by Sinopharm Chemical Reagent Company, and selected with purities higher than 99.5% to calibrate the designed densitometer. A kerosene type of endothermic hydrocarbon fuel(EHF-1) distilled from petroleum was chosen and tested. The detailed descriptions of all samples were listed in Table 1. EHF-1 fuel consists of 81.40% cycloalkanes, 4.75% alkanes, 4.88% alkenes, and 4.00% aromatics, with minor amounts of olefins, naphthalenes, and other hydrocarbons [14]. Critical parameters of EHF-1 were $T_c$=694.1 K, $p_c$=2.35 MPa, which was obtained by the critical opalescence phenomena in a visualization apparatus [15].

**Table 1** Description of Samples

| Chemical name | source | initial mole fraction purity | purification method |
|---|---|---|---|
| hexane | Sinopharm Chemical Reagent Company | 0.995 | distillation |
| heptane | Sinopharm Chemical Reagent Company | 0.995 | distillation |
| octane | Sinopharm Chemical Reagent Company | 0.995 | distillation |
| nitrogen | Sinopharm Chemical Reagent Company | 0.998 | none |
| EHF-1 | kerosene fuel | | distillation |

## METHODOLOGY AND PROCEDURE

The densitometer is based on the fact the gamma ray attenuated when it passed though the test tube which was filled with measured fluid. The intensity of the gamma ray decreased exponentially, which was govern by the Beer–Lambert's law

$$I=I_0 \exp[-(\mu/\rho)\cdot\rho x] \quad (1)$$

where $I$, $I_0$, $\mu/\rho$, $\rho$ and $x$ represent for the intensity of incident radiation, the intensity of detected radiation, mass absorption coefficient, the density of the absorption materials and the distance between the radiation source and detected scintillator, respectively. A high density and a low density fluid are obtained from references [13,16].

Firstly, a high density fluid flowed through the test section. The relation is

$$I_{\mathrm{H}} = I_0 \exp\left[-(\mu/\rho)_{\mathrm{H}} \rho_{\mathrm{H}} x\right] \cdot \left[-(\mu/\rho)_{\mathrm{w}} \rho_{\mathrm{w}} x_w\right] \tag{2}$$

Then, a low density fluid was filled with the test section. The relation is given as

$$I_{\mathrm{L}} = I_0 \exp\left[-(\mu/\rho)_{\mathrm{L}} \rho_{\mathrm{L}} x\right] \cdot \left[-(\mu/\rho)_{\mathrm{w}} \rho_{\mathrm{w}} x_w\right] \tag{3}$$

Finally, the measured fluid flowed through the test section. The relation is expressed as

$$I_{\mathrm{m}} = I_0 \exp\left[-(\mu/\rho)_{\mathrm{m}} \rho_{\mathrm{m}} x\right] \cdot \left[-(\mu/\rho)_{\mathrm{w}} \rho_{\mathrm{w}} x_w\right] \tag{4}$$

Equations 2 to 4 can be combined to obtain a logarithmic relation given as

$$\ln\left(\frac{I_{\mathrm{H}}}{I_{\mathrm{L}}}\right) = \left(-\mu/\rho\right)_{\mathrm{H}} \rho_{\mathrm{H}} x - \left(-\mu/\rho\right)_{\mathrm{L}} \rho_{\mathrm{L}} x \tag{5}$$

$$\ln\left(\frac{I_{\mathrm{H}}}{I_{\mathrm{m}}}\right) = \left(-\mu/\rho\right)_{\mathrm{H}} \rho_{\mathrm{H}} x - \left(-\mu/\rho\right)_{\mathrm{m}} \rho_{\mathrm{m}} x \tag{6}$$

Then the above two formulas are combined to a relation as follows:

$$\ln\left(\frac{I_{\mathrm{H}}}{I_{\mathrm{L}}}\right) / \ln\left(\frac{I_{\mathrm{H}}}{I_{\mathrm{m}}}\right) = \frac{\left(-\mu/\rho\right)_{\mathrm{H}} \rho_{\mathrm{H}} - \left(-\mu/\rho\right)_{\mathrm{L}} \rho_{\mathrm{L}}}{\left(-\mu/\rho\right)_{\mathrm{H}} \rho_{\mathrm{H}} - \left(-\mu/\rho\right)_{\mathrm{m}} \rho_{\mathrm{m}}} \tag{7}$$

Because the ingredients of the measured and high density fluid are almost the same [13,14], the values of the mass absorption coefficient are equal. The density of low density fluid is far less than the density of measured and high density fluid. So, the mass absorption of low density fluid is neglected. The count rate of the densitometer is proportion to the intensity of the radiations. The final relation of the theory formula can be given as

$$\rho_{\mathrm{m}} = \rho_{\mathrm{H}} - \rho_{\mathrm{H}} \cdot \frac{\ln(\Phi_{\mathrm{m}} / \Phi_{\mathrm{H}})}{\ln(\Phi_{\mathrm{L}} / \Phi_{\mathrm{H}})} \tag{8}$$

where $\Phi$, $\Phi_{\mathrm{H}}$ and $\Phi_{\mathrm{L}}$ are the count of the measured fluid, high and low density fluid. The density of the measured fluid can be obtained by the measured count rate of the fluid and referenced data with different densities, whose range consists of the test density.

## UNCERTAINTIES ANALISIS

According to equation (8), the combined relative standard uncertainty of the measured density $u_{\mathrm{r}}(\rho_{\mathrm{m}})$

$$\begin{aligned} u_{\mathrm{r}}^2(\rho_{\mathrm{m}}) = {} & u_{\mathrm{r}}^2(\rho_{\mathrm{H}}) + u_{\mathrm{r}}^2(\rho_{\mathrm{L}}) + u_{\mathrm{r}}^2\left(\frac{\phi_{\mathrm{m}}}{\phi_{\mathrm{H}}}\right) + u_{\mathrm{r}}^2\left(\frac{\phi_{\mathrm{L}}}{\phi_{\mathrm{H}}}\right) \\ & + \left(\frac{\partial \rho_{\mathrm{m}}}{\partial T} \cdot \frac{u(T)}{\rho_{\mathrm{m}}}\right)^2 + \left(\frac{\partial \rho_{\mathrm{m}}}{\partial p} \cdot \frac{u(p)}{\rho_{\mathrm{m}}}\right)^2 \end{aligned} \tag{9}$$

Here, $u_{\mathrm{r}}(X)$ is the combined relative standard uncertainty and $u(X)$ is the standard uncertainty of variable $X$. In this work, the uncertainties of the main parameters have been listed in Table 2. Each pressure transducer was calibrated by a pressure calibrator supplied by Mesor Ltd. The platinum resistance thermometers were calibrated by a JOFRA temperature calibrator. Thus, the combined standard uncertainty of density is calculated as (0.13 to 1.46) %.

## CALIBRATION

The intensity of gamma ray has been absorbed partially by the wall of test tube when it passed through the test section. The dependence of the count rate on the ambient and test pipe temperature was examined. As Figure 3 showed, the count rate was nearly constant with the temperature range from 235.0 K to 353.0 K, which indicated that a weak dependency on the temperature due to the protection of the thermal shielding and heat isolation on the test pipe.

**Table 2** Uncertainties of the main experimental parameters.

| Parameters | Factor of uncertainty | Maximum uncertainty |
|---|---|---|
| Mass flow rate | Combined standard uncertainty | 0.0012g/s |
| Pressure | Combined standard uncertainty | 0.03MPa |
| Temperature | Combined standard uncertainty | 0.022K |
| $\phi_{\mathrm{L}}/\phi_{\mathrm{M}}$ | Combined relative standard uncertainty | 0.41% |
| $\phi_{\mathrm{L}}/\phi_{\mathrm{H}}$ | Combined relative standard uncertainty | 0.32% |
| $\rho_{\mathrm{H}}$ | Combined standard uncertainty | 0.1g/cm$^3$ |
| $\rho_{\mathrm{L}}$ | Combined standard uncertainty | 0.01g/cm$^3$ |

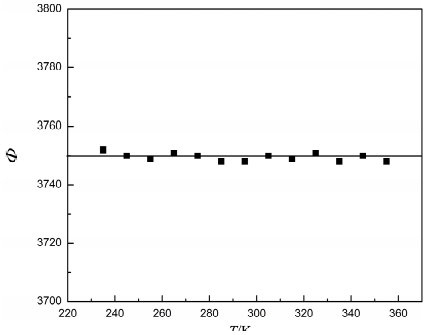


**Figure 3** Dependency of the count rate on the temperature

The validity of the densitometer was verified by measuring the

densities of hexane at 3.07 MPa. The binary mixture of n-heptane and n-octane were further tested. Densities of the referenced fluids measured in experiments were compared with the data available at NIST and references [16,17]. In calculation, the percentage deviation (PD), the average absolute deviation (AAD) and the maximum absolute deviation (MAD) of the results were defined:

$$\mathrm{PD}=\left(\frac{\rho_{\mathrm{exp}}}{\rho_{\mathrm{ref}}}-1\right)\times 100\% \tag{10}$$

$$\mathrm{AAD}=\frac{\sum_{\mathrm{i}=1}^{\mathrm{n}}\mathrm{abs}(PD_i)}{\mathrm{n}} \tag{11}$$

$$\mathrm{MAD}=\max(\mathrm{abs}(PD_{\mathrm{i}})) \tag{12}$$

Experimental densities of hexane were measured at $T$= （233.0-353.0） K and $p$=3.07 MPa. Good agreement was achieved in Table 3 and Figure 4. The MAD is within 0.67 % and the AAD is within 0.32 %. The results indicated the reliability of densitometer in pure substance is conformed.

**Table 3** Experimental values and referenced data of density $\rho$ at temperature $T$, pressure $p$ and relative differences $\rho=（\rho_{\mathrm{exp}}-\rho_{\mathrm{ref}})/\rho_{\mathrm{ref}}$ for the hexane [α]

| $T$ | $\rho_{\mathrm{exp}}$ | $\rho_{\mathrm{ref}}$ | $\frac{\Delta\rho}{\rho}$ | $T$/K | $\rho_{\mathrm{exp}}$ | $\rho_{\mathrm{ref}}$ | $\frac{\Delta\rho}{\rho}$ |
|---|---|---|---|---|---|---|---|
| K | kg.cm$^{-3}$ | kg.cm$^{-3}$ | % | K | kg.cm$^{-3}$ | kg.cm$^{-3}$ | % |
| | | | $p$=3.07 MPa | | | | |
| 233.1 | 711.9 | 715.0 | 0.43 | 303.1 | 653.7 | 653.7 | 0.01 |
| 242.9 | 703.3 | 706.3 | 0.42 | 313.0 | 647.3 | 644.7 | -0.40 |
| 253.0 | 694.2 | 697.7 | 0.67 | 323.1 | 637.2 | 635.5 | -0.28 |
| 263.2 | 690.4 | 689.0 | -0.20 | 332.9 | 627.7 | 626.1 | -0.25 |
| 273.0 | 684.5 | 680.3 | -0.62 | 343.1 | 618.0 | 616.6 | -0.23 |
| 283.1 | 671.2 | 671.5 | 0.05 | 353.0 | 611.0 | 606.9 | -0.38 |
| 292.9 | 664.2 | 662.7 | -0.24 | | | | |

[α] Standard uncertainties $u$ are $u(T)$=0.02 K ,$u(p)$=0.03 MPa and the combined expanded uncertainty $U_{\mathrm{c}}$ is $U_{\mathrm{c}}(\rho)$=1.8 kg.m$^{-3}$ (0.95 level of confidence).

The densities of w=0.28 n-heptane and w= 0.72 n-octane mixture were measured at a constant pressure 0.10 MPa with temperature from (293.1 to 343.1) K. The results are compared with the values available at reference [17] as shown in Table 4 and Figure 5. The MAD is limited to 0.60% and the AAD was 0.28%. The excellent agreement confirms the accuracy of the densitometer for binary mixtures, which illustrating that densitometer could be applied to the multi-component mixtures measurement. Thus, the densities of a kind endothermic hydrocarbon fuel were measured at different pressures in the following part.

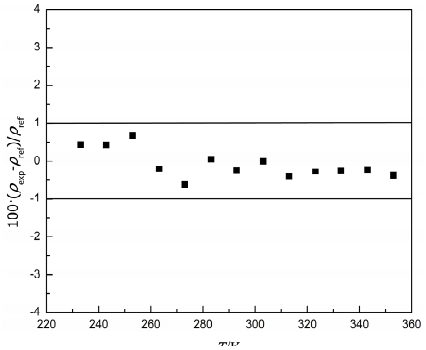


**Figure 4** Deviations of measured and referenced densities of hexane versus temperature at $p$ = 3.07 MPa**.**

**Table 4** Experimental values and referenced data of density $\rho$ at temperature $T$, pressure $p$ and relative differences $\rho=（\rho_{\mathrm{exp}}-\rho_{\mathrm{ref}})/\rho_{\mathrm{ref}}$ for the heptane and octane mixture [α]

| $T$ | $\rho_{\mathrm{exp}}$ | $\rho_{\mathrm{ref}}$ | $\frac{\Delta\rho}{\rho}$ | $T$/K | $\rho_{\mathrm{exp}}$ | $\rho_{\mathrm{ref}}$ | $\frac{\Delta\rho}{\rho}$ |
|---|---|---|---|---|---|---|---|
| K | kg.cm$^{-3}$ | kg.cm$^{-3}$ | % | K | kg.cm$^{-3}$ | kg.cm$^{-3}$ | % |
| | | | $w$=0.28 heptane and $w$=0.72 octane | | | | |
| | | | $p$=0.10 MPa | | | | |
| 293.2 | 699.8 | 697.8 | -0.29 | 318.2 | 673.3 | 677.4 | 0.60 |
| 298.2 | 694.8 | 694.0 | -0.11 | 323.2 | 675.0 | 673.2 | -0.28 |
| 303.2 | 692.2 | 689.9 | -0.34 | 333.2 | 666.6 | 664.9 | -0.25 |
| 308.2 | 689.4 | 686.1 | -0.48 | 338.2 | 659.5 | 661.0 | 0.23 |
| 313.2 | 678.3 | 681.6 | 0.48 | 343.2 | 656.5 | 656.8 | 0.05 |

[α] Standard uncertainties $u$ are $u(T)$=0.02 K, $u(p)$=0.03 MPa and the combined expanded uncertainty $U_{\mathrm{c}}$ is $U_{\mathrm{c}}(\rho)$=1.75 kg.m$^{-3}$ (0.95 level of confidence)。

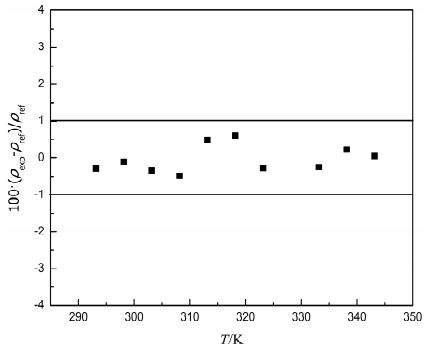


**Figure 5** Deviations of measured and referenced densities of heptane and octane mixture versus temperature at $p$ = 0.10MPa**.**

## DENSITY OF HYDROCARBON FUEL

Densities of endothermic hydrocarbon fuel were measured covering a temperature range of (335.0-353.0) K at pressures of (0.68,1.47,3.06 and 4.09) MPa. The data was shown in Table 5 and the variation of densities was presented in Figure 6. The fuel was a liquid state in the measured range. In the working condition, the density decreased as the temperature increased and the fuel was a incompressible fluid, so the pressure had little effect on the density of fuel. The fuel's densities were compared with the referenced data calculated by Yaws [18] and deviation between the calculated densities and experimental data were shown in Figure 7, where the overall relative deviations were within 1.96 %.

**Table 5** Experimental values of density $\rho$ at temperature $T$, pressure $p$ for the fuel [α]

| $T$ | $\rho_{exp}$ | $T$ | $\rho_{exp}$ | $T$ | $\rho_{exp}$ | $T$ | $\rho_{exp}$ |
|---|---|---|---|---|---|---|---|
| K | kg.cm$^{-3}$ | K | kg.cm$^{-3}$ | K | kg.cm$^{-3}$ | K | kg.cm$^{-3}$ |
| $p$=0.68MPa | | $p$=1.47MPa | | $p$=3.06MPa | | $p$=4.09MPa | |
| 235.8 | 834.4 | 235.8 | 835.3 | 235.8 | 836.9 | 235.4 | 838.1 |
| 245.2 | 829.3 | 245.4 | 830.8 | 245.2 | 831.3 | 245.2 | 832.2 |
| 254.2 | 824.1 | 254.3 | 824.9 | 254.2 | 825.8 | 254.2 | 826.9 |
| 263.4 | 819.0 | 263.3 | 820.3 | 263.4 | 821.4 | 263.4 | 822.3 |
| 272.5 | 813.9 | 272.6 | 815.0 | 272.5 | 815.8 | 272.5 | 816.4 |
| 281.6 | 808.8 | 281.5 | 809.8 | 281.6 | 810.6 | 281.6 | 811.1 |
| 290.5 | 803.7 | 290.4 | 804.5 | 290.5 | 804.9 | 290.5 | 805.8 |
| 300.1 | 798.6 | 300.2 | 800.0 | 300.1 | 800.9 | 300.1 | 801.6 |
| 309.3 | 793.5 | 309.2 | 794.3 | 309.3 | 795.1 | 309.3 | 796.1 |
| 318.4 | 788.4 | 318.2 | 789.1 | 318.4 | 790.3 | 318.4 | 791.1 |
| 327.1 | 782.7 | 327.2 | 783.5 | 327.1 | 784.9 | 327.1 | 785.8 |
| 336.3 | 777.0 | 336.3 | 778.1 | 336.3 | 778.9 | 336.3 | 779.4 |
| 345.9 | 771.3 | 345.9 | 772.5 | 345.9 | 773.9 | 345.9 | 775.1 |
| 355.2 | 766.6 | 355.3 | 767.1 | 355.2 | 767.9 | 355.2 | 768.8 |

[α] Standard uncertainties $u$ are $u(T)$=0.02 K , $u(p)$=0.03 MPa and the combined expanded uncertainty $U_c$ is $U_c(\rho)$=2.2 kg.m$^{-3}$ (0.95 level of confidence).

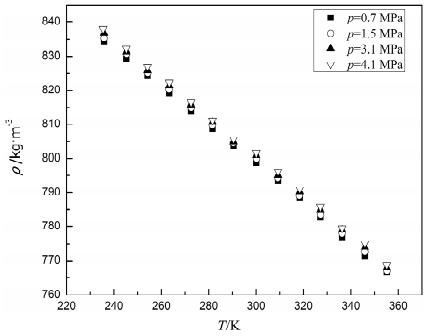


Figure 6 Density variation of fuel versus temperature

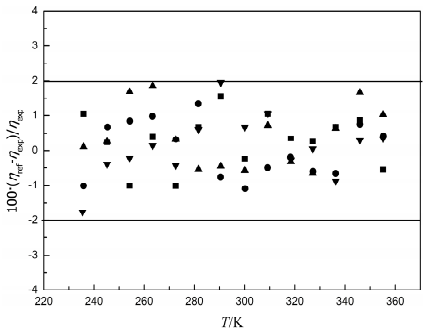


**Figure 7** ■,relative deviations $\Delta\eta/\eta = (\eta_{ref} - \eta_{exp})/\eta_{exp}$ at $p$ = 0.68 MPa; ●,relative deviations $\Delta\eta/\eta = (\eta_{ref} - \eta_{exp})/\eta_{exp}$ at $p$ = 1.47 MPa;▲,relative deviations $\Delta\eta/\eta = (\eta_{ref} - \eta_{exp})/\eta_{exp}$ at $p$ = 3.06 MPa;▼,relative deviations $\Delta\eta/\eta = (\eta_{ref} - \eta_{exp})/\eta_{exp}$ at $p$ = 4.09 MPa.

## CONCLUSION

The densities of endothermic hydrocarbon fuels were measured at temperatures from (235.0 to 353.0) K and at pressures of (0.68,1.47, 3.06 and 4.09) MPa. Pure hexane and a binary mixture of n-heptane and n-octane were adopted respectively to validate the reliability and accuracy of the densitometer. Results showed the average absolute deviation(AAD) was lower than 0.32 % and the maximum absolute deviation(MAD) was within 0.67 %. The aim of this study is to provide new experimental data to complete the non-experimental data region.

## REFERENCES

[1] Edwards T., Cracking and deposition behavior of supercritical hydrocarbon aviation fuels, *Combustion Science and Technology*, Vol. 178, 2006, pp.307-334

[2] David R.S., and Spadaccini L.S., Hydrocarbon Fuel Cooling Technologies for Advanced Propulsion, *ASME 1995 International Gas Turbine and Aeroengine Congress and Exposition*, Vol. 3, 1995, pp.344-351

[3] Lander H., and Nixon A.C., Endothermic Fuels for Hypersonic Vehicles, *Journal of Aircraft*, Vol. 8, 1971, pp. 200-207

[4] Fujiwara K., Nakamura K., and Noguchi M., Critical parameters and vapor pressure measurements for 1,1,1-trifluoroethane (R-143a), *Journal of Chemical &Engineering Data*, Vol.43, 1998,pp.55-59

[5] Meng X.Y., Zheng P.J., Wu J.T., and Liu Z.G., Density and viscosity measurements of diethyl ether from 243 to 373 K and up to 20MPa, *Fluid Phase Equilibria,* Vol.271, 2008,pp.1-5

[6] Lei Y.T., Chen Z.Y., An X.Q., Huang M.J., and Shen W.G., Measurements of density and heat capacity for binary mixtures {$x$ benzonitrile + (1 −$x$) (octane or nonane)}, *Journal of Chemical &Engineering Data*, Vol.55,2010,pp. 4154–4161

[7] Narendra K., Krishna T.S., Sudhamsa B., Dey R., and Sarathbabu

M., Thermophysical and optical studies of molecular interactions in binary mixtures of diethyl carbonate with aromatic compounds at temperatures from 298.15 to 323.15 K, *The Journal of Thermophysical Dynamics,* Vol.103, 2016,pp. 17–29

[8] Miyamoto H., Koshi T., and Uematsu M., The ($p$, $\rho$, $T$, $x$) properties for (propane + $n$-butane + isobutane) ternary mixtures over the temperature range from (280 to 440) K at pressures from (1 to 200) MPa, *The Journal of Chemical Thermodynamics*,Vol.40, 2008,pp. 558–566

[9] Abdulagatov I.M., and Azizov N.D., ($p$,$\rho$,$T$,$x$) and viscosity measurements of {$x_1$$n$-heptane + (1 − $x_1$)$n$-octane} mixtures at high temperatures and high pressures, *The Journal of Chemical Thermodynamics*, Vol.38, 2006, pp. 1402–1415

[10] Stringari P., Scalabrin G., and Richon D., Liquid density measurements for the propylene + 2-propanol + water system, *Journal of Chemical &Engineering Data*, Vol.54, 2009, pp.2285–2290

[11] Nikitin E.D., Pavlov P.A., and Skripov P.V., Measurement of the critical properties of thermally unstable substances and mixtures by the pulse-heating method, *The Journal of Chemical Thermodynamics*, Vol.25, 1993, pp. 869-880

[12] Deng J.W., Zhang C.B., Xu G.Q., Tao Z., Zhang B., and Liu G.Z., Density measurements of endothermic hydrocarbon fuel at sub- and supercritical conditions, *Journal of Chemical &Engineering Data*, Vol.56, 2011, pp.2980-2986

[13] Yang Z.Q., Bi Q.C., Guo Y., Liu Z.H., Yan J.G., and Zhang Q., Design of a gamma densitometer for hydrocarbon fuel at high temperature and supercritical pressure, *Journal of Chemical &Engineering Data*, Vol.59, 2014, pp. 3335–3343

[14] Yang Z.Q., Liu Z.H., Bi Q.C., Feng S., Pan H., and Guo Y., Viscosity measurements of hydrocarbon fuel at temperatures from (303.2 to 513.2) K and pressures up to 5.1 MPa using a two-capillary viscometer, *Thermochimic Acta*, Vol.617, 2015, pp.1-7

[15] He M.G.,Xin N., Liu Y., and Zhang Y., Determination of critical properties for binary and ternary mixtures of short chain alcohols and alkanes using a flow apparatus, *The Journal of Supercritical Fluids*, Vol.104, 2015, pp.19-28

[16] Lemmon E. W., Huber M. L., and McLinden M. O., NIST Standard Reference Database 23, NIST Reference Fluid Thermodynamic and Transport Properties, REFPROP version 9.0, Standard Reference Data Program, *National Institute of Standards and Technology*, Gaithersburg, MD, 2010

[17] Abdulagatov I.M., and Azizov N.D., ($p$,$\rho$,$T$,$x$) and viscosity measurements of {$x_1$$n$-heptane + (1 − $x_1$)$n$-octane} mixtures at high temperatures and high pressures, *The Journal of Chemical Thermodynamics*, Vol.38,2006, pp. 1402–1415

[18] Yaws C.L., Thermophysical properties of chemicals and hydrocarbons, *Wlliam Andrew*,2014